Vol. 82: 253–264, 2019
https://doi.org/10.3354/ame01895

AQUATIC MICROBIAL ECOLOGY
Aquat Microb Ecol

Published online January 21

Benthic microalgal variability associated with peritidal stromatolite microhabitats along the South African coast

Ross-Lynne A. Weston[1,*], Renzo Perissinotto[1], Gavin M. Rishworth[1], Paul-Pierre Steyn[2]

[1]DST/NRF Research Chair in Shallow Water Ecosystems, Institute for Coastal and Marine Research (CMR), Nelson Mandela University, Port Elizabeth 6031, South Africa

[2]Department of Botany, Nelson Mandela University, Port Elizabeth 6031, South Africa

ABSTRACT: Stromatolites, structures formed with the input of microorganisms such as cyanobacteria, can be traced back to the Precambrian. Many modern marine stromatolites have a coarser internal structure and host a diverse eukaryotic community. Known as eualgal–cyanobacterial stromatolites, these formations are likely a result of the higher abundance of larger sediment particles from the biomineralisation of skeletal material. However, it is unclear how eukaryotic microalgae have contributed towards modern stromatolite formation. Therefore, the aim of this study was to investigate how the microalgal community contributes towards the differences in depth profiles and layering observed amongst mesofabric structures in stromatolite pools along the Port Elizabeth coastline in South Africa. This goal was achieved by comparing the proportional abundances of each of the major microalgal classes (cyanobacteria, bacillariophytes and chlorophytes) between the different mesofabric types and depth profiles. Clear variability in terms of proportional abundance was apparent between microhabitats and with depth. Coarser, irregular types had a higher bacillariophyte biomass than smoother types. This difference is likely a consequence of the greater efficiency of bacillariophytes in trapping larger sediment particles. Eukaryotic microalgae (specifically bacillariophytes) are highlighted as important ecosystem engineers in these modern ecosystems.

KEY WORDS: Microbialites · Mesofabric types · Niches · Microphytobenthos · Ecosystem engineering

INTRODUCTION

Modern living marine stromatolites have previously been thought of as partial analogues to fossilised stromatolites and have persisted since the Precambrian (Dupraz & Visscher 2005, Baumgartner et al. 2009, Dupraz et al. 2009). However, in contrast to their ancient counterparts, many modern examples have a coarser internal structure and host a community of eukaryotic microalgae (Feldmann & Mckenzie 1998, Frantz et al. 2015). Larger sediment particles are difficult to trap by cyanobacteria, which have fine filaments. The radiation (evolutionary divergence from an ancestor) of eukaryotic microalgae that are capable of trapping larger sand grains resulted in the modern (post-Miocene) coarse-grained formations known as eualgal–cyanobacterial stromatolites (Pratt 1982, Awramik & Riding 1988, Frantz et al. 2015). These modern formations host a more complex mixed community made up of cyanobacteria, eukaryotic microalgae such as bacillariophytes, and in some cases macroalgae (Neumann & Scoffin 1970, Awramik & Riding 1988, Frantz et al. 2015). These organisms all play a role in the building and maintenance of these formations.

*Corresponding author: rosslynne.weston747@gmail.com

Defined as laminated organosedimentary growths (Awramik 1976, Semikhatov et al. 1979), stromatolite construction is initiated by the trapping and binding of sediment that is lithified by the deposition of inorganic carbonates (Reid et al. 2000, Dupraz et al. 2009). This usually follows a successional pattern within the microalgal community, observed as 3 typical stages (Reid et al. 2000). Type 1, pioneer mats, are dominated by filamentous cyanobacteria (Reid et al. 2000); Type 2 mats contain fewer cyanobacteria but have a higher diversity of heterotrophic organisms and bacillariophytes than that found in Type 1 mats (Reid et al. 2000, Decho et al. 2005); Type 3 mats form the climax communities of stromatolite formations (Reid et al. 2000). During a hiatus, which is responsible for succession to a Type 2 or Type 3 mat, micritic crusts are formed by carbonate deposition.

Riding et al. (1991) suggested that microalgal groups may differ between microhabitats. More cryptic species are found in pockets and spaces between bound sand grains, whereas other species may extend into the water column through filaments or stalks (Allwood et al. 2006). Stalk formation, motility by means of exopolymeric substances (EPS) and epiphytic behaviour allow microalgae to cope with the light attenuation associated with burial in sediment (Allwood et al. 2006). Although differing amongst microbialite habitats, successional changes in the microbial community between cyanobacteria and bacillariophyte groups are driven by variable environmental pressures, such as salinity or inundation (Bowlin et al. 2012, Suosaari et al. 2016). In addition to temporal, successional shifts in the microalgal community, spatial variability in terms of community composition has also been observed amongst different stromatolite mesofabric structures (Jahnert & Collins 2011, Suosaari et al. 2016).

However, the role of different microalgae in terms of creating microhabitats within stromatolite formations has not been thoroughly investigated. In peritidal tufa stromatolites that were recently discovered along the South African coastline (Smith et al. 2011, Perissinotto et al. 2014), a number of mesofabric structural types have been recognised (Perissinotto et al. 2014, Edwards et al. 2017). These stromatolites form at the interface of carbonate-rich groundwater seepage (Dodd et al. 2018) and ocean inflow, thereby constructing peritidal, barrage (sensu Forbes et al. 2010) pools bordered by the accreting stromatolite matrix (Rishworth et al. 2017a). Although featuring limited columnar growth structures compared to their better-known counterparts in Shark Bay, Australia, and the Bahamas (e.g. Suosaari et al. 2016), the characteristic stromatolite layering defining these microbialites (sensu Reid et al. 2000) is nonetheless evident and well documented (Perissinotto et al. 2014, Rishworth et al. 2016, Edwards et al. 2017). Within the peritidal stromatolites, colloform growths are observed in the deeper sections of the pools, predominantly submerged (Perissinotto et al. 2014). They are recognised as cauliflower-like mounds with an irregular surface and support an abundant bacillariophyte assemblage (Suosaari et al. 2016). Laminar (or smooth) deposits, which have well-defined layering, are found along the edges of barrage pools and host a diverse cyanobacterial community (Jahnert & Collins 2012, Perissinotto et al. 2014, Suosaari et al. 2016). Pustular formations are found in the shallow water around the rims of barrage pools or at waterfall formations (Perissinotto et al. 2014). These mesofabric types have also been observed at Giant's Causeway, Ireland (Cooper et al. 2013), Shark Bay, Australia (Reid et al. 2003, Suosaari et al. 2016) and Cape Morgan, South Africa (Smith & Uken 2003, Smith et al. 2005), and have been shown to vary in terms of the metazoan community they support (Weston et al. 2018).

The aim of this study was to investigate how the microalgal community contributes to the differences observed amongst mesofabric structures in terms of depth profiles and layering. We hypothesised that (1) the majority of the microalgal biomass would be confined to the surface layer of the mat and (2) coarse-grained mesofabric types would have a higher microalgal biomass, with bacillariophytes being a dominant component compared to those types with a fine-grained, well-laminated structure.

MATERIALS AND METHODS

Study site

The study was undertaken at 3 stromatolite sites along the Port Elizabeth coastline (Fig. 1), located west of Cape Recife (Site A; 34° 02′ 42.13″ S, 25° 34′ 07.50″ E), at Schoenmakerskop (Site B; 34° 02′ 28.23″ S, 25° 32′ 18.60″ E) and Seaview (Site C; 34° 01′ 03.16″ S, 25° 21′ 56.48″ E, South Africa). The stromatolites found at these localities are of the barrage-type tufa mats (Forbes et al. 2010, Perissinotto et al. 2014). Port Elizabeth mesofabric types were classified (Fig. 2) prior to sampling based on those described in previous studies (Reid et al. 2003, Jahnert & Collins 2012, Cooper et al. 2013, Suosaari et al. 2016, Edwards et al. 2017).

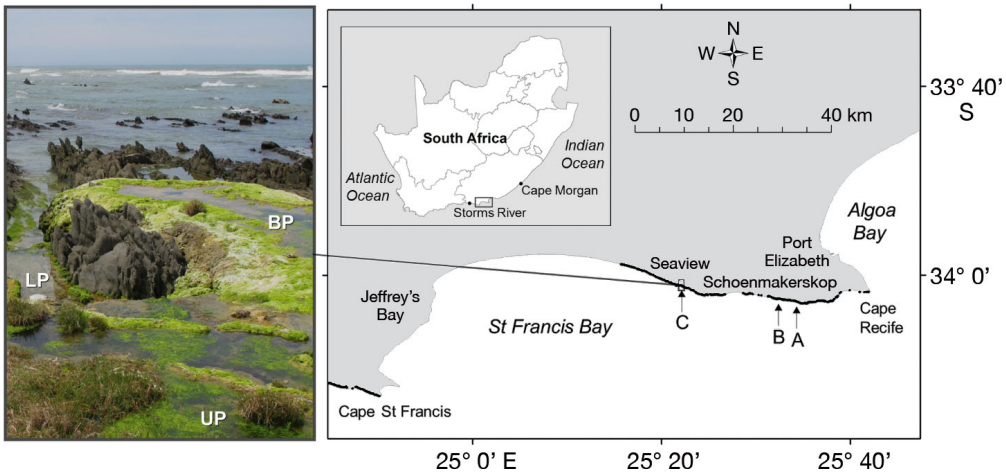

Fig. 1. The 3 stromatolite sites sampled (A, B, C), including the location of all coastal freshwater seeps from Cape Recife to Oyster Bay (black dots, 540 in total). Adapted from Rishworth et al. (2017c). The photograph on the left shows a typical stromatolite accretion (at Seaview, Site C), demonstrating the relative pool locations: LP: lower pool; BP: barrage pool; UP: upper pool

Physico-chemistry

To account for inter-site variability, physico-chemical parameters were measured in the main pool at each site using a YSI 6600-V2 multiprobe system. The parameters measured were temperature, salinity (PSU or ‰), depth, pH, turbidity (NTU) and dissolved oxygen (mg l^{-1}). Photosynthetically active radiation (PAR) was also measured at the sediment–water interface and just below the water surface of the main pool at each site using a light meter (LI-250A; LICOR) fitted with a LI-193SA underwater spherical quantum sensor. Water samples were collected from each pool for nutrient analysis. These were filtered through Whatman GF/F glass-fibre filters (1.0 µm) and the filtrates frozen in 150 ml bottles. The samples were analysed for ammonium, nitrate and nitrite (dissolved inorganic nitrogen, DIN) and soluble reactive phosphorus (dissolved inorganic phosphorus, DIP) using standard spectrophotometric methods (described in Rishworth et al. 2017a).

Microalgal community trends

Sediment cores were collected during the 2 climatic seasons in the region: September 2015 (end of winter) and January 2016 (mid-summer). Three replicate cores, to a depth of 30 mm, were collected from each of the mesofabric types (from the main pool) at each site using a stainless steel corer (17 mm internal diameter), and thereafter sectioned into three 10 mm depth layers. These were collected in tandem with those of Weston et al. (2018) to minimise sampling disturbance.

Relative percentage composition of algal classes (cyanobacteria, chlorophytes and bacillariophytes) in each core section was measured *in situ* using a BenthoTorch (bbe Moldaenke). This device uses the differences in fluorescence response patterns between microalgal taxa as a tool for measuring the proportional concentrations of cyanobacteria, bacillariophytes and chlorophytes (Aberle et al. 2006). Different microalgal groups emit characteristic fluorescence signatures based on their accessory pigments (Beutler et al. 2002, Aberle et al. 2006). The BenthoTorch detects these signatures and provides a relative rather than absolute proportion of each algal class (Aberle et al. 2006). The BenthoTorch, like many *in situ* fluorescence instruments, is limited in terms of accuracy by the physiological variability in fluorescence signatures emitted (i.e. chlorophyll fluorescence relative to cell size), taxon-specific quenching patterns which cause biases, and interference from chromophores (Macintyre et al. 2010). However, the primary advantage is that broad, real-time and *in situ* patterns in relative abundance between differing taxa can be detected and studied (MacIntyre et al. 2010). This was deemed a necessary trade-off (i.e. between accuracy and overall trend estimation) in the stromatolite habitats whereby minimal extensive disturbance through destructive sampling on these sensitive ecosystems was essential. This technique has been used successfully for these stromatolites and has been verified in preliminary tests (this study: n = ~15 cores) to qualitatively align with conventionally measured (*ex situ* under a Zeiss Leica DMLL inverted microscope) microalgal taxonomic patterns (see Perissinotto et al. 2014, Rishworth et al. 2016). However, it must be noted in terms of result interpretation that the data presented are reflective of relative microalgal trends rather absolute abundance estimates. Furthermore, the BenthoTorch usually eliminates all surrounding light when taking a

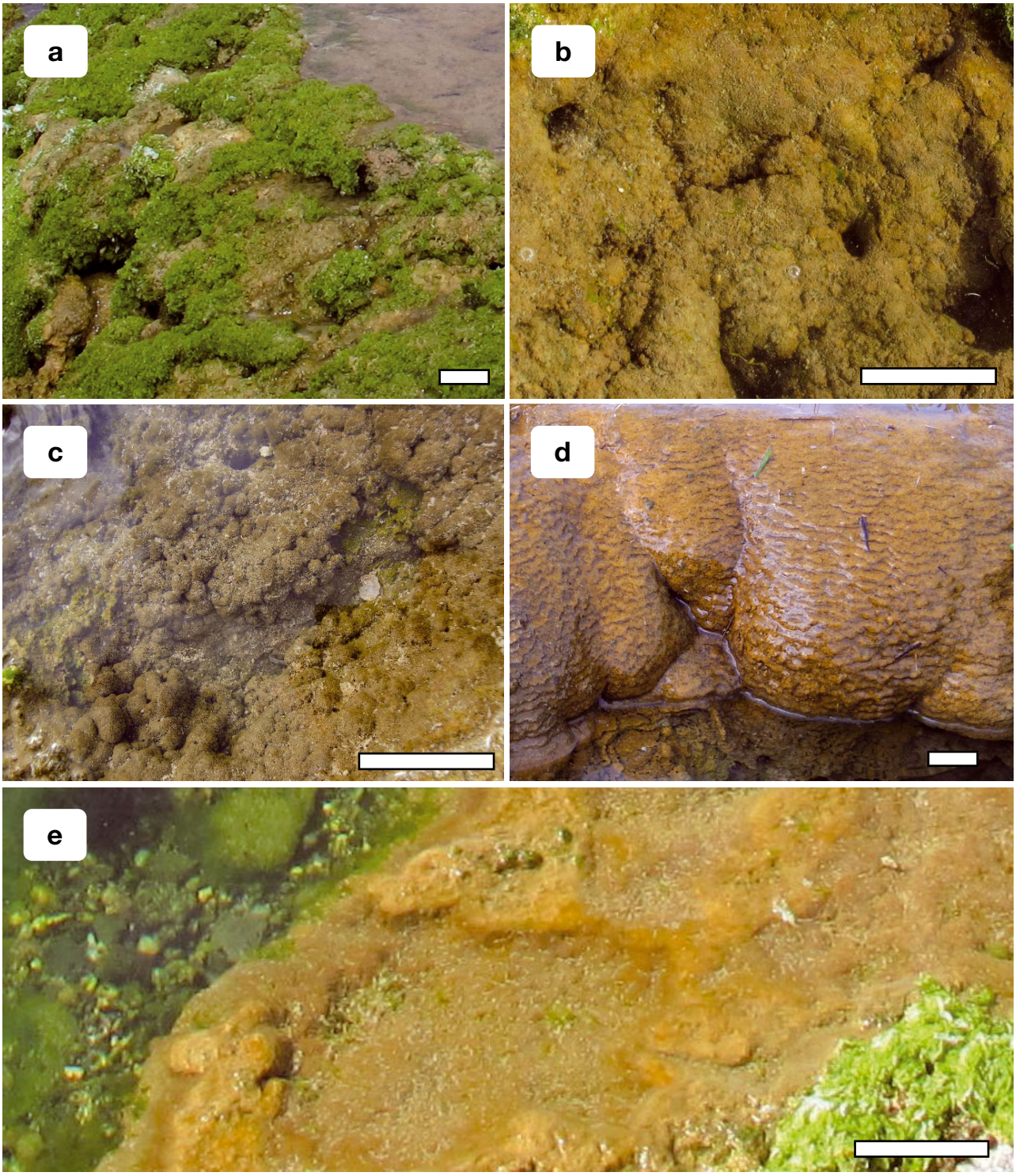

Fig. 2. Mesofabric types identified at the stromatolite locations along the South African coastline. (a) Rimstone is found at the rims of barrage pools, generally exposed; structures are irregularly clotted and can be covered in dense macroalgal mats. (b) Pustular is found in the shallow parts of barrage pools (<15 cm depth); generally porous, with marked bioturbation often visible. (c) Colloform occurs in the deeper sections and along walls of barrage pools; globular and botryoidal in appearance. (d) Wrinkled laminar forms on slopes, often associated with waterfalls; wavy appearance; usually dark brown in colour. (e) Laminar flat, also known as 'smooth', occurs on flat sections usually adjacent to barrage pool rims; shiny and smooth in appearance; light brown in colour. As examples of their global distribution, rimstone and wrinkled laminar types have been documented from Western Australia (Forbes et al. 2010) while all other types have been observed at Giant's Causeway, Ireland (Cooper et al. 2013) and at Shark Bay, Australia (Reid et al. 2003, Suosaari et al. 2016). Scale bars = 5 cm. Photographs taken by Lynette Clennell. Reproduced from Weston et al. (2018)

measurement, using a delay-timer to dark-acclimate the sampled area, thereby minimising the unwanted effect of nonphotochemical quenching on the fluorescence signal of the sample (Beutler et al. 2002, Aberle et al. 2006, MacIntyre et al. 2010).

A polyethylene bottle was cut in half and covered in duct tape to avoid ambient light interference. Each 10 mm section of each core was then positioned into the bottle vertically and measured individually with the BenthoTorch. The cores did break apart on occasion, but this was shown in preliminary tests to not affect the measurement of proportional microalgae composition. Each core section was then placed in a 30 ml solution of 90% acetone for 48 h to extract chlorophyll *a* (chl *a*) and phaeopigments. Fluorescence readings were measured on a Turner 10-AU narrow-band system (Turner Designs). The BenthoTorch proportions obtained were used to calculate the percentage contribution of each class to the total chl *a* (acetone extracted fluorescence measurements).

Grain size

Grain size analysis was done by measuring the sizes of approximately 150–200 grains per sample (as in Tarhan et al. 2013). This was done using a Nikon SMZ 25 stereomicroscope with a camera attached. Each grain was measured using the microscope camera software. An analysis of variance (ANOVA) was done to test for grain size differences between mesofabric types.

Data analysis

Variance inflation factors (VIFs) of the potential predictor variables were used to assess collinearity. The interaction of grain size with core depth was collinear with both core depth and grain size (VIF 6.45). Mesofabric type with grain size was collinear with both mesofabric type and grain size (VIF 4.49). The interactions of grain size with core depth as well as mesofabric type with grain size were therefore removed from the analyses, after which the remaining variables were statistically independent (VIF < 3.5) (Zuur et al. 2009).

The contribution of each algal class to the total chl *a* extracted was expressed as a proportion based on the BenthoTorch measurements (Rishworth et al. 2016). The data were analysed in R (R Core Team 2018) using the multivariate abundance analysis package 'mvabund'. This package, based on the generalised linear model (GLM) framework, has been shown to be more powerful than community analysis distance-based methods (Wang et al. 2012, Warton et al. 2012). By fitting a separate model to each taxon, the mean variance relationship can be modelled more accurately using this method, by accounting for the change in variability between the different taxa (Warton et al. 2012). The function 'manyglm' was used to fit a GLM to the algal class community data (10 000 iterations). Predictor variables included in the model were site, season, grain size, mesofabric type and core depth. Microalgal classes were compared between predictors using a repeated-measures ANOVA and residuals were assessed for normality and heterogeneity. Data are presented as mean ± SD.

RESULTS

Physico-chemical water parameters (Table 1) varied little between sites and seasons. Temperature, turbidity and DIP were higher in summer compared to winter, whereas the other measured parameters were all higher in winter (Table 1). Nutrient and salinity measurements reflected the most apparent

Table 1. Physico-chemical water parameters recorded at 3 stromatolite pools along the South African coastline near Port Elizabeth during September 2015 (end of winter) and January 2016 (summer). DO: dissolved oxygen; PAR: photosynthetically active radiation; DIN: dissolved inorganic nitrogen; DIP: dissolved inorganic phosphorus

	Temperature (°C)	Salinity	pH	DO (mg l^{-1})	Turbidity (NTU)	PAR (µmol m^{-2} s^{-1})	DIN (µM)	DIP (µM)
Site								
A	21.02 ± 0.59	1.27 ± 0.08	8.49 ± 0.13	17.44 ± 2.81	0.00 ± 0.00	863.00 ± 82.32	42.47 ± 7.37	0.12 ± 0.05
B	21.44 ± 0.81	2.90 ± 0.99	8.61 ± 0.28	10.09 ± 2.71	0.65 ± 0.65	491.05 ± 87.87	216.84 ± 33.04	0.15 ± 0.06
C	20.02 ± 1.28	6.66 ± 4.37	8.51 ± 0.54	6.90 ± 2.12	0.00 ± 0.00	253.85 ± 32.55	478.87 ± 87.53	0.52 ± 0.06
Season								
Summer	21.46 ± 0.55	2.23 ± 0.68	8.21 ± 0.12	8.94 ± 1.99	0.43 ± 0.43	457.37 ± 170.48	223.31 ± 53.45	0.40 ± 0.06
Winter	20.37 ± 0.71	4.09 ± 2.29	8.86 ± 0.21	15.77 ± 2.90	0.00 ± 0.00	614.57 ± 104.22	268.80 ± 0.06	0.13 ± 0.06

site-related differences (Table 1). Although the salinity of Sites A and B reflect that of oligohaline conditions (1.27 ± 0.08 and 2.90 ± 0.99, respectively) and Site C reflects that of mesohaline conditions (6.66 ± 4.73), site-related differences were not reflected in the microalgal community (Tables 1 & 2).

Cyanobacteria showed the highest benthic microalgal biomass overall and Chlorophyta the least (Fig. 3). Core depth was significantly correlated (GLM: $p < 0.01$) with microalgal community dynamics (Table 2). All 3 microalgal classes (cyanobacteria, chlorophytes and bacillariophytes) reflected a similar trend where the highest biomass was found in the first, upper cm and decreased with depth (Fig. 3). Mesofabric type overall was not important (GLM: $p > 0.05$) in describing community dynamics (Table 2). However, when interacting with core depth, a strong correlation (GLM: $p < 0.01$) was evident as a predictor of community dynamics (Table 2).

Mesofabric type was only a significant predictor for bacillariophyte biomass ($p < 0.05$) compared to the other algal groups (Tables 2 & 3). Bacillariophyte biomass was significantly related to both mesofabric type ($p < 0.05$) and depth ($p < 0.01$) as well as the interaction thereof, whereas cyanobacteria and Chlorophyta biomass were only significantly related ($p < 0.01$) to core depth (Tables 2 & 3) and the interaction of core depth and mesofabric type, respectively.

Overall, microalgal biomass was highest in the rimstone type, followed by colloform, and lowest in the laminar flat type (Fig. 4). Cyanobacteria were more abundant in the colloform type and lowest in the laminar flat mats (Fig. 5). The well-laminated and fine-grained wrinkled laminar mesofabric showed an increase in cyanobacterial abundance in summer. Bacillariophytes had the highest biomass in the rimstone type ($p < 0.01$; Table 3, Fig. 5). Otherwise there were no seasonal differences in microalgae biomass between the different mesofabric types.

The first centimetre of core depth reflected the highest biomass in the rimstone type and the lowest in the laminar flat type (Fig. 6). The microalgal biomass between mesofabric types in the lower depths differed from that found in the upper cm (highest biomass in colloform type and lowest biomass in rimstone and laminar types). The deepest centimetre

Table 2. Overall multivariate generalised linear model, showing significance levels for test statistics (p) and deviance (*D*) explained for the main parameters tested, for each microalgal class at 3 stromatolites pools along the South African coastline near Port Elizabeth during September 2015 (end of winter) and January 2016 (summer)

Parameter	Overall model			Algal classes					
				Chlorophyta		Cyanobacteria		Bacillariophyta	
	df	p	*D*	p	*D*	p	*D*	p	*D*
Mesofabric type	4	0.07	41.00	0.40	6.32	0.40	7.56	0.02	27.07
Depth	1	<0.01	214.35	<0.01	130.81	<0.01	51.79	<0.01	31.75
Grain size	1	1.00	0.06	1.00	0.01	1.00	0.03	1.00	0.02
Season	1	0.88	0.60	0.92	0.29	0.92	0.26	0.92	0.05
Site	2	0.38	7.60	0.99	0.01	0.19	6.34	0.75	1.24
Mesofabric type: depth	4	<0.01	62.49	0.11	9.43	<0.01	25.28	<0.01	27.77

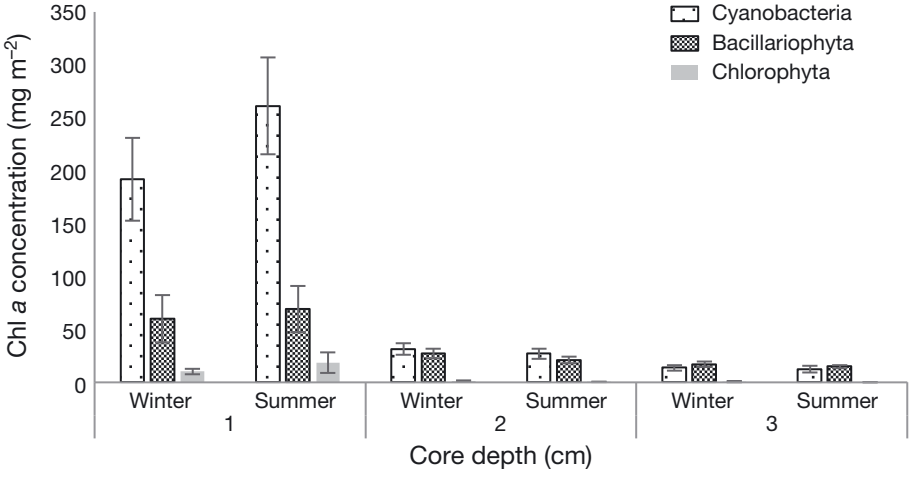

Fig. 3. Overall mean chl *a* concentration according to depth for all mesofabric types at 3 stromatolite pools (averaged across sites) along the South African coastline near Port Elizabeth during September 2015 (end of winter) and January 2016 (summer)

Table 3. Generalised linear model of parameters tested for each microalgal class at 3 stromatolite pools along the South African coastline near Port Elizabeth during September 2015 (end of winter) and January 2016 (summer). Significance levels for Wald test statistics (p) and model coefficients (*C*) for all predictors for class-specific univariate models are indicated. Coefficients for mesofabric type, season and site are shown relative to their reference categories ('Colloform', 'Summer' and 'Site A', respectively, as shown by the superscript label)

Parameters	Algal classes					
	Chlorophyta		Cyanobacteria		Bacillariophytes	
	p	*C*	p	*C*	p	*C*
Intercept	<0.01	13.54 ± 85.46	<0.01	6.75 ± 0.49	<0.01	4.27 ± 0.46
Laminar flat	0.79	−0.33 ± 121.17	0.27	−0.74 ± 0.58	0.09	−1.17 ± 0.55
Pustular	0.91	−11.38 ± 85.46	0.98	<0.01 ± 0.57	0.37	0.66 ± 0.54
Rimstone	0.28	−7.49 ± 85.47	0.29	0.64 ± 0.58	<0.01	2.33 ± 0.54
Wrinkled laminar	0.89	−11.63 ± 85.46	0.87	−0.25 ± 0.57	0.89	−0.07 ± 0.54
Depth	0.09	−13.20 ± 85.46	<0.01	−1.24 ± 0.19	0.09	−0.33 ± 0.18
Grain size	0.40	0.01 ± <0.01	0.97	<0.01 ± <0.01	0.97	<−0.01 ± <0.01
Season^{Winter}	0.88	0.19 ± 0.30	0.88	−0.10 ± 0.14	0.91	−0.01 ± 0.13
Site^{B}	0.03	1.23 ± 0.42	0.88	−0.02 ± 0.18	0.11	−0.34 ± 0.17
Site^{C}	0.08	0.96 ± 0.39	0.86	−0.03 ± 0.18	0.24	−0.25 ± 0.16
Laminar flat: depth	0.79	0.15 ± 121.17	0.58	−0.20 ± 0.28	0.58	0.23 ± 0.26
Pustular: depth	0.50	11.71 ± 85.46	0.5	−0.19 ± 0.27	0.31	−0.34 ± 0.25
Rimstone: depth	0.02	8.87 ± 85.46	0.02	−0.71 ± 0.28	<0.01	−1.07 ± 0.26
Wrinkled laminar: depth	0.90	11.54 ± 85.46	0.8	−0.12 ± 0.27	0.93	−0.02 ± 0.25

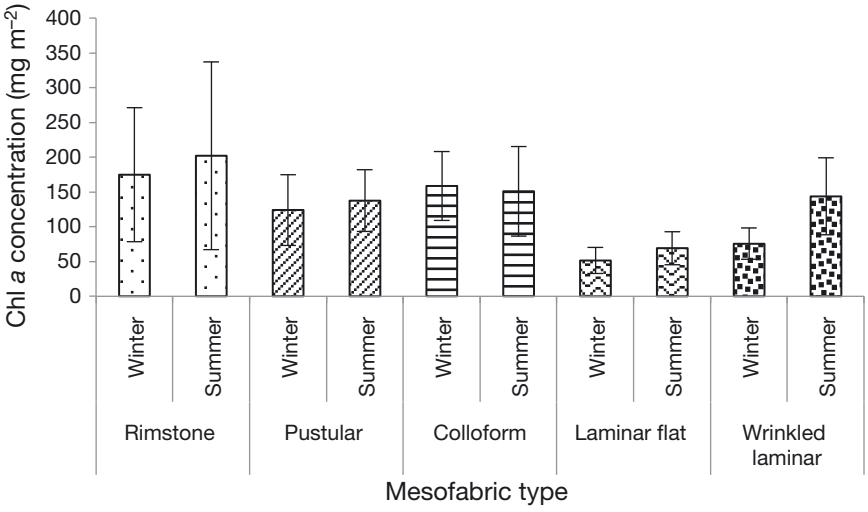

Fig. 4. Overall mean chl *a* concentration measured for each mesofabric type at 3 stromatolite (averaged across sites) pools along the South African coastline near Port Elizabeth during September 2015 (end of winter) and January 2016 (summer)

had very low algal biomass, and differences between mesofabric types were small.

Although grain size was not a significant correlate to the distribution of any of the microalgal classes ($p > 0.05$), grain size measurements were significantly different between mesofabric types (ANOVA, $p = 0.0064$). Overall, the rimstone mesofabric contained comparatively larger grains than the other types. Pustular mats, although similar to the other types, contained more smaller grains (Fig. S1 in the Supplement at www.int-res.com/articles/suppl/a082p253_supp.pdf). All the microhabitats contained a higher percentage of very fine sediment (65–125 µm) and silt (<65 µm) than larger particles (>125 µm). The percentage of larger sediment was higher in winter than in summer for all the types except rimstone. The rimstone type had the highest percentage of the larger sediment particles, whereas the other types had more silt particles, with all mesofabrics displaying an approximately normal frequency distribution in grain sizes (Figs. S1 & S2, Table S3).

DISCUSSION

Coarse-grained stromatolites with disrupted layering are hypothesised to be formed with input from eukaryotic microalgal taxa, such as bacillariophytes

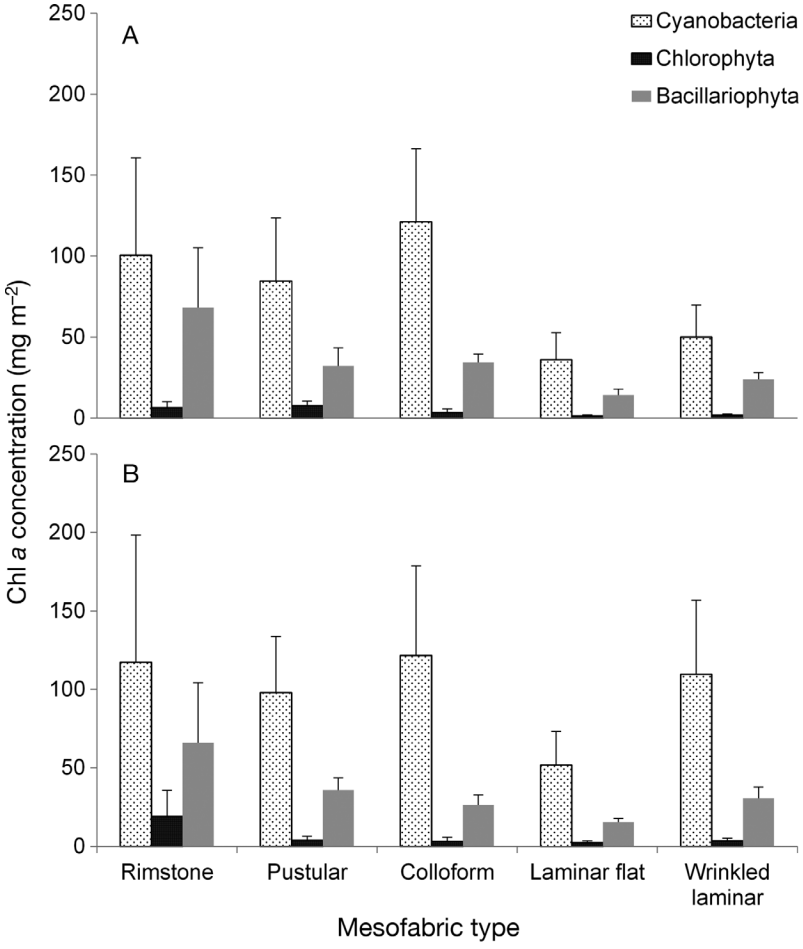

Fig. 5. Mean chl *a* concentration of each algal class measured for each mesofabric type at 3 stromatolite pools (averaged across sites) along the South African coastline near Port Elizabeth during (A) September 2015 (end of winter) and (B) January 2016 (summer)

and chlorophytes (Awramik & Riding 1988, Riding et al. 1991, Hoagland et al. 1993, Tice et al. 2011, Frantz et al. 2015). Rishworth et al. (2016) demonstrated that in addition to cyanobacteria, bacillariophytes are a dominant component of the benthic microalgal biomass within the Port Elizabeth stromatolites. While the surface layers of stromatolite accretion support the bulk of the microalgal (cyanobacteria and bacillariophytes) biomass (Smith et al. 2011, Rishworth et al. 2016), this study shows that microalgal community composition also varies with depth amongst different mesofabric types (Table 2). Although known to occur in addition to cyanobacteria, eukaryotic microalgae such as bacillariophytes are capable of trapping and binding much larger sediment particles than cyanobacteria through EPS production (Awramik & Riding 1988, Frantz et al. 2015). Therefore, coarse-grained, disrupted formations (such as rimstone, colloform and pustular) are expected to have a higher overall microalgal biomass, and specifically more bacillariophytes, than the more fine-grained formations (laminar flat and wrinkled laminar). In the results presented in this study, coarser mesofabric types (rimstone, colloform and pustular) did have a higher microalgal biomass. This was also demonstrated by Suosaari et al. (2016), where colloform and pustular formations had a higher biomass (as well as more bacillariophyte enrichment) compared to smooth formations.

A gradual transition of microalgal communities between different mesofabric types has previously been observed in Shark Bay, where there is a higher diversity in the upper intertidal types (particularly pustular) than in those found in the intertidal or subtidal areas (particularly smooth and colloform) (Suosaari et al. 2016). Given that the mesofabric types in the main stromatolite pool at each site in Port Elizabeth do not differ in elevation, the drivers of structural differences are likely different from those experienced in Shark Bay. Geological research done in Port Elizabeth on mesofabric types showed that rimstone tufa forms first, where freshwater collects in surface depressions in the bedrock and starts to overflow (Edwards et al. 2017). The rims grow and thicken, trapping freshwater in the pool and supporting pustular and colloform growth within (Edwards et al. 2017). The microbial community echoes this observation, as demonstrated by the high abundance of microalgae in rimstone formations, followed by pustular and colloform. The rimstone mesofabric type, which reflected a higher abundance of larger sediment grains, also had the highest overall biomass and the highest abundance of bacillariophytes. Given that bacillariophytes are capable of trapping larger sediment grains, it is unsurprising that the higher biomass would be found in the coarser mesofabric type. Bacillariophytes are also capable of stabilising sediments, and it has been noted that mats made up of only cyanobacteria eroded more readily and had lower productivity than those which hosted a bacillariophyte–cyanobacteria community (Neumann & Scoffin 1970, Perkins et al. 2012).

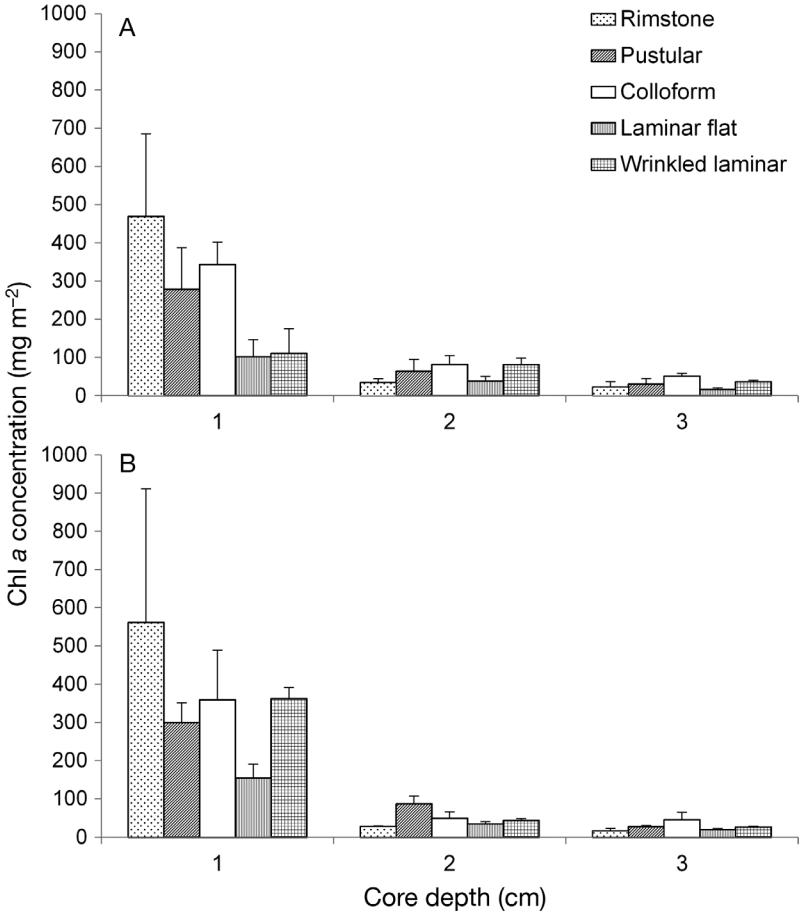

Fig. 6. Mean chl *a* concentrations for each mesofabric type at each core depth at 3 stromatolite pools (averaged across sites) along the South African coastline near Port Elizabeth during (A) September 2015 (end of winter) and (B) January 2016 (summer)

This is informative, in that the comparatively higher bacillariophyte biomass in the rimstone type is likely a result of its position relative to the incoming tide and storm-surge wave energy, given the stronger sediment-stabilising properties of this taxon. The rimstone walls are a critical component to the system, as they trap nutrients, calcium carbonate and sediments within the barrage pool (Rishworth et al. 2016), allowing the formation of the other microhabitats. These walls also create a barrier or buffer against the force of the incoming tide and storm surges. Marine flooding, which occurs in this system at spring high tides, likely introduces bacillariophytes into the system (Rishworth et al. 2017b).

Pustular formations host the second largest bacillariophyte community. It is likely that the unconsolidated appearance of the pustular mats is a result of the high bacillariophyte abundance which traps larger grains. Given the proximity of pustular mats to rimstone, as well as the high bacillariophyte abundance, these mats essentially form as an extension or transition of the rimstone walls. In contrast to the bacillariophyte-dominated formations, colloform formations have the highest cyanobacterial abundance. These deposits form cauliflower-like mounds and are found along the sides of the pools, usually on an incline. The surface of these mounds is rough with adjoining globules, making up the cauliflower-like shape and forming crevices (Edwards et al. 2017). The combination of a larger surface area, rough surface and crevices likely allows sediment (contained within the barrage pool) to be trapped long enough to be bound by cyanobacteria and mucilaginous bacillariophytes, and subsequently, precipitation can occur (Awramik & Riding 1988, Riding et al. 1991, Frantz et al. 2015).

The wrinkled laminar formations host a lower bacillariophyte abundance than the aforementioned type, but the wrinkles likely trap sediment or at least slow down the movement of sediments washed over the surface of the mat by overflow water exiting the pools (Frantz et al. 2015). This type, together with the laminar flat formations, appears to have a film over the surface which may be excess EPS produced by the microalgae. This film is likely integral to trapping sediments, thereby creating these two formations. As highlighted in the literature, EPS is produced by microorganisms for various purposes such as motility or stalk formation (Allwood et al. 2006). The production of EPS is particularly important for trapping sediments on an incline (for example, for wrinkled laminar) (Awramik & Riding 1988). EPS is not only important in trapping sediment, but also in carbonate deposition. The degradation of EPS releases calcium ions into the surrounding water, which supports precipitation of calcium carbonate (Dupraz et al. 2009). The lower bacillariophyte abundance in the wrinkled laminar and laminar flat types is indicative that they are less important to the building of these mesofabrics than cyanobacteria when compared to coarser types. The laminar flat mesofabric type, being the most fine-grained formation, is the closest representative within the Port Elizabeth stromatolites of those from the Precambrian in terms of

community composition and lamination (Awramik & Riding 1988, Riding et al. 1991).

Although there are more microalgae observed in summer than in winter for all microhabitats, except colloform, season was not an important component in the model. There were, however, interesting differences in grain sizes between the 2 seasons. The rimstone type had a higher percentage of sand than silt or fine sediment in summer than in winter. The opposite was observed for all the other types, with more silt in summer, more sand in winter and a higher percentage of smaller grain sizes. This can be attributed to the higher frequency of seawater flooding in winter (Rishworth et al. 2017a), which introduces larger sediments into the pool. However, the spread of the different size classes was more even in rimstone than the other types. The overall percentages for silt and very fine sand were much higher than for sand. Tarhan et al. (2013) compared grain sizes between different mat types in Exuma Cays, Bahamas (Table S2). Their study showed that mean grain size was slightly higher in coarser mats than in finer, well-laminated mats. However, the mean grain sizes are much larger in the Bahamas than at the sites examined here. Although Port Elizabeth has larger grains (Tables S1 & S3), these are lower in abundance within the stromatolite mats compared to smaller particles. This is either a consequence of an overall lower abundance of these larger grains or a lower abundance of these grains incorporated into these mats. Instructively, the peritidal mat (Type D) which was described by Tarhan et al. (2013) has a closer mean grain size to those observed in the present study. This, coupled with the higher mean grain size in the rimstone type (closer to the sea), suggests that position along the shore may be important in terms of grain size, as the stromatolites explored in this study were in peritidal systems.

The transition between different microbial communities is likely linked to micro-environmental factors within each mat type (Bowlin et al. 2012, Perkins et al. 2012). Previous studies investigating community changes between different successional mat types have shown that photosynthetically active cyanobacteria dominate Type 1 mats, followed by a less productive Type 2 mat, which is where carbonate deposition occurs and micritic crusts are formed (Reid et al. 2000, Perkins et al. 2012). After a prolonged pause in sediment accretion, the surface of microbial mats is colonised by eukaryotes and is highly productive (Reid et al. 2000, Bowlin et al. 2012, Perkins et al. 2012). Although bacillariophytes are important in the trapping of sediment when sedimentation is resumed, it is the cyanobacteria that are responsible for the precipitation of calcium carbonate to form lithified mats (Awramik & Riding 1988, Dupraz et al. 2009). The association of bacillariophytes and cyanobacteria results in a highly productive community in the rimstone walls, allowing for rapid pioneer growth (Edwards et al. 2017).

Recognising the methodological limitations imposed in this study (i.e. relative rather than absolute estimations of microalgal community composition using the BenthoTorch), these results nonetheless make a useful contribution in terms of the interplay between diatoms (eukaryotes) and cyanobacteria with respect to microbialite formation. In doing so, this study highlights the importance of the contribution of bacillariophytes towards constructing the coarser mesofabric types of stromatolite formations by trapping larger sediment grains. The microalgae in this system act as ecosystem engineers by building the rimstone dams, which enables the concentration of nutrients (Rishworth et al. 2017a) and calcium carbonate (Dodd et al. 2018) that are essential to the development of the other mesofabric types. These microhabitats likely provide variable niches for colonisation by metazoan organisms (Weston et al. 2018). Future studies should investigate these dynamics at a finer taxonomic resolution, accounting for the destructive nature of this sampling. Currently, only the genera of the cyanobacterial community are known in part, comprising taxa such as *Lyngbya*, *Leptolyngbya*, *Plectonema* and *Schizothrix* (Perissinotto et al. 2014), while the chlorophytes and diatoms remain to be properly characterised. A comprehensive metagenomic assessment of the microbial community at these sites is currently underway as part of a separate study. Additionally, it would be interesting to investigate which accessory photosynthetic pigments cyanobacteria from these stromatolites possess. For example, it was in the stromatolites of Shark Bay where chlorophyll *f* was first observed (Chen at al. 2010). This information would likely play an important role in further understanding microhabitat variability and construction between mesofabrics, as well as the bottom-up effects on coexisting metazoans in terms of refugia dynamics (Weston et al. 2018).

Acknowledgements. The National Research Foundation (NRF; Scarce skills Masters Scholarship, Grant UID: 100009) and the Nelson Mandela University (Postgraduate Research Scholarships) are acknowledged for the personal funding awarded to R.A.W. This research was funded by the Department of Science and Technology (DST) and the NRF, under the DST-NRF South African Research Chairs Initiative (SARChI), in Shallow Water Ecosystems (Grant UID: 84375). The opinions expressed, and conclusions arrived at, are

those of the authors, and are not necessarily to be attributed to the NRF or Nelson Mandela University. The Claude Leon Foundation is thanked for the Postdoctoral Fellowship provided to G.M.R. Three anonymous reviewers are thanked for their useful comments which helped improve this manuscript.

LITERATURE CITED

Aberle N, Beutler M, Moldaenke C, Wiltshire KH (2006) 'Spectral fingerprinting' for specific algal groups on sediments *in situ*: a new sensor. Arch Hydrobiol 167:1–4

Allwood AC, Walter MR, Kamber BS, Marshall CP, Burch IW (2006) Stromatolite reef from the early Archaean era of Australia. Nature 441:714–718

Awramik SM (1976) Gunflint stromatolites: microfossil distribution in relation to stromatolite morphology. Dev Sedimentol 20:311–320

Awramik SM, Riding R (1988) Role of algal eukaryotes in subtidal columnar stromatolite formation. Proc Natl Acad Sci USA 85:1327–1329

Baumgartner LK, Spear JR, Buckley DH, Pace NR, Reid RP, Dupraz C, Visscher PT (2009) Microbial diversity in modern marine stromatolites, Highborne Cay, Bahamas. Environ Microbiol 11:2710–2719

Beutler M, Wiltshire KH, Meyer B, Moldaenke C and others (2002) A fluorometric method for the differentiation of algal populations *in vivo* and *in situ*. Photosynth Res 72: 39–53

Bowlin EM, Klaus JS, Foster JS, Andres MS, Custals L, Reid RP (2012) Environmental controls on microbial community cycling in modern marine stromatolites. Sediment Geol 263-264:45–55

Chen M, Schliep M, Willows RD, Cai ZL, Neilan BA, Scheer H (2010) A red-shifted chlorophyll. Science 329: 1318–1319

Cooper A, Smith A, Arnscheidt J (2013) Contemporary stromatolite formation in high intertidal rock pools, Giant's Causeway, Northern Ireland: preliminary observations. J Coast Res 65:1675–1680

Decho AW, Visscher PT, Reid RP (2005) Production and cycling of natural microbial exopolymers (EPS) within a marine stromatolite. Palaeogeogr Palaeoclimatol Palaeoecol 219:71–86

Dodd C, Anderson CR, Perissinotto R, du Plooy SJ, Rishworth GM (2018) Hydrochemistry of peritidal stromatolite pools and associated freshwater inlets along the Eastern Cape Coast, South Africa. Sediment Geol 373: 163–179

Dupraz C, Visscher PT (2005) Microbial lithification in marine stromatolites and hypersaline mats. Trends Microbiol 13:429–438

Dupraz C, Reid RP, Braissant O, Decho AW, Norman RS, Visscher PT (2009) Processes of carbonate precipitation in modern microbial mats. Earth Sci Rev 96:141–162

Edwards MJK, Anderson CR, Perissinotto R, Rishworth GM (2017) Macro- and meso-fabric structures of peritidal tufa stromatolites along the Eastern Cape coast of South Africa. Sediment Geol 359:62–75

Feldmann M, Mckenzie JA (1998) Stromatolite-thrombolite associations in a modern environment, Lee Stocking Island, Bahamas. Palaios 13:201–212

Forbes M, Vogwill R, Onton K (2010) A characterisation of the coastal tufa deposits of south-west Western Australia. Sediment Geol 232:52–65

Frantz CM, Petryshyn VA, Corsetti FA (2015) Grain trapping by filamentous cyanobacterial and algal mats: implications for stromatolite microfabrics through time. Geobiology 13:409–423

Hoagland KD, Rosowski JR, Gretz MR, Roemer SC (1993) Diatom extracellular polymeric substances: function, fine structure, chemistry, and physiology. J Phycol 29(5): 537–566

Jahnert RJ, Collins LB (2011) Significance of subtidal microbial deposits in Shark Bay, Australia. Mar Geol 286: 106–111

Jahnert RJ, Collins LB (2012) Characteristics, distribution and morphogenesis of subtidal microbial systems in Shark Bay, Australia. Mar Geol 303-306:115–136

MacIntyre HL, Lawrenz E, Richardson TL (2010) Taxonomic discrimination of phytoplankton by spectral fluorescence. In: Suggett DJ, Prášil O, Borowitzka MA (eds) Chlorophyll *a* fluorescence in aquatic sciences: methods and applications. Springer, Dordrecht, p 129–169

Neumann AC, Scoffin TP (1970) The composition, structure and erodability of subtidal mats, Abaco, Bahamas. J Sediment Petrol 40:274–297

Perissinotto R, Bornman TG, Steyn PP, Miranda NAF and others (2014) Tufa stromatolite ecosystems on the South African south coast. S Afr J Sci 110:89–96

Perkins RG, Mouget JL, Kromkamp JC, Stolz J, Reid PR (2012) Modern stromatolite phototrophic communities: a comparative study of procaryote and eucaryote phototrophs using variable chlorophyll fluorescence. FEMS Microbiol Ecol 82:584–596

Pratt BR (1982) Stromatolite decline — a reconsideration. Geology 10:512–515

Reid RP, Visscher PT, Decho AW, Stolz JF and others (2000) The role of microbes in accretion, lamination and early lithification of modern marine stromatolites. Nature 406: 989–992

Reid RP, James NP, Macintyre IG, Dupraz CP, Burne RV (2003) Shark Bay stromatolites: microfabrics and reinterpretation of origins. Facies 49:299–324

Riding R, Awramik SM, Winsborough BM, Griffin KM, Dill RF (1991) Bahamian giant stromatolites: microbial composition of surface mats. Geol Mag 128:227–234

Rishworth GM, van Elden S, Perissinotto R, Miranda NAF, Steyn PP, Bornman TG (2016) Environmental influences on living marine stromatolites: insights from benthic microalgal communities. Environ Microbiol 18:503–513

Rishworth GM, Perissinotto R, Bornman TG, Lemley DA (2017a) Peritidal stromatolites at the convergence of groundwater seepage and marine incursion: patterns of salinity, temperature and nutrient variability. J Mar Syst 167:68–77

Rishworth GM, Perissinotto R, Miranda NAF, Bornman TG, Steyn PP (2017b) Phytoplankton community dynamics within peritidal pools associated with living stromatolites at the freshwater–marine interface. Aquat Sci 79:357–370

Rishworth GM, Perissinotto R, Bird MS (2017c) Patterns and drivers of benthic macrofaunal communities dwelling within extant peritidal stromatolites. Limnol Oceanogr 62:2227–2242

Semikhatov MA, Gebelein CD, Cloud P, Awramik SM, Benmore WC (1979) Stromatolite morphogenesis — progress and problems. Can J Earth Sci 16:992–1015

Smith AM, Uken R (2003) Living marine stromatolites at Kei River mouth. S Afr J Sci 99:200

Smith AM, Uken R, Thackeray Z (2005) Cape Morgan peritidal stromatolites: the origin of lamination. S Afr J Sci 101:107–108

Smith AM, Andrews JE, Uken R, Thackeray Z, Perissinotto R, Leuci R, Marca-Bell A (2011) Rock pool tufa stromatolites on a modern South African wave-cut platform: Partial analogues for Archaean stromatolites? Terra Nova 23:375–381

Suosaari EP, Reid RP, Playford PE, Foster JS and others (2016) New multi-scale perspectives on the stromatolites of Shark Bay, Western Australia. Sci Rep 6:20557

Tarhan LG, Planavsky NJ, Laumer CE, Stolz JF, Reid RP (2013) Microbial mat controls on infaunal abundance and diversity in modern marine microbialites. Geobiology 11:485–497

Tice MM, Thornton DC, Pope MC, Olszewski TD, Gong J (2011) Archean microbial mat communities. Annu Rev Earth Planet Sci 39:297–39

Wang Y, Naumann U, Wright ST, Warton DI (2012) mvabund — an R package for model-based analysis of multivariate abundance data. Methods Ecol Evol 3: 471–474

Warton DI, Wright ST, Wang Y (2012) Distance-based multivariate analyses confound location and dispersion effects. Methods Ecol Evol 3:89–101

Weston RLA, Perissinotto R, Rishworth GM, Steyn PP (2018) Macroinvertebrate variability between microhabitats of peritidal stromatolites along the South African coast. Mar Ecol Prog Ser 605:37–47

Zuur AF, Ieno EN, Walker NJ, Saveliev AA, Smith GM (2009) Mixed effects models and extensions in ecology with R. Springer, New York, NY

Editorial responsibility: Zoe Finkel, Sackville, New Brunswick, Canada

Submitted: February 1, 2018; Accepted: October 26, 2018
Proofs received from author(s): December 10, 2018